On Lab Test of Coherence in Event Horizon Imager

V. Kudriashov, M. Martin-Neira, E. Lia, P. Jankovic,
D/TEC
ESTEC ESA
Noordwijk, Netherlands
Volodymyr.Kudriashov@esa.int

J. Michalski, P. Kant, D. Trofimowicz

SpaceForest
Gdynia, Poland
Jerzy.Michalski@spaceforest.pl

***Abstract*—Event horizon imaging requires a third-generation space Very Long Baseline Interferometer on a 500 GHz band. The interferometer challenges available frequency standards. Namely, the practical coherent integration time is about 45 times shorter than needed. A self-calibration could aid this though a 3rd satellite is needed hence, an increased mission cost. This paper is devoted to experimental verification of a novel concept for two-way frequency transfer.**

We built a dedicated breadboard, test set-up, and run tests with and without temperature differences between branches of the breadboard. A phase difference between derived oscillators is the white noise-like function of the time with 1-σ of 0.5° at 103.2 GHz over more than 3 hours. Varying the temperature difference between branches ±3 C during 4.5 hours, being the orbit period, confirmed that the phase difference is the function of this temperature difference too. The Allan Deviation demonstrated between two derived 103.2 GHz oscillators is of $1.1\times10^{-14}/\tau$ over 10 ms < τ < 1000 s, where τ is the averaging time, and the optical communication link path length is 5 km (17 ms). Degradation of this Allan Deviation is of 2 times at the longest-possible delay of 0.2 s in the interferometer system; the 0.2 s is the biggest sum of geometric and communication delays. This worst-case satisfies the requirement with a margin of *11 times*. An obtained coherence is in the range of 0.997–0.9998 which is beneficial for the interferometer, at 557 GHz. This is one of the key technology enablers for black hole imaging from space.

Keywords—breadboard; frequency transfer; interferometry; very long baseline interferometry; space

I. INTRODUCTION

Sagittarius A* is a bright object of a big angular size and well-known mass and hence, it is a handy object for the gravity theory choice [1]. An angular resolution required on its image is of 5 micro arc seconds (μas). Very Long Baseline Interferometry (VLBI) is the only way to deliver it.

The lowest-possible frequency which allows *both* mitigating the scattering by interstellar electrons in the Galactic plane (which would distort the image of the Sagittarius A*) and imaging planet-forming disks, is 557 GHz [1]. Tropospheric phase corruptions would challenge such a high-frequency interferometer. A distance between telescopes needed to deliver the 5 μas is 25,000 km. Hence, space VLBI.

Independent individual oscillators cannot assure the coherent operation of such a high-frequency interferometer. Jennison phase closure may solve the issue, though the minimum number of required telescope satellites is three, a notable cost increase over an imager consisting of only two [1]. This is why a frequency transfer between two satellites is addressed.

With single-piece dish antennas limited to circa 4 m diameter to fit into the launch vehicle, both the integration time required for detection and the time for obtaining a high-quality image are technically challenging. Therefore, an alternative concept of interferometry is followed. The concept utilizes telescope-satellites in Polar Medium Earth Orbits involving inter-satellite optical links for local oscillator connection between the satellites, data transfer and metrology. This approach is dubbed Event Horizon Imager, EHI. This connection realizes the symmetric two-way frequency transfer concept as shown in Fig. 5 of [2]. The concept achieves coherent local oscillators at the two satellites and alleviates the need for the knowledge accuracy of the inter-satellite velocity for the transfer. We built a dedicated breadboard to test it.

The paper reports a both dedicated breadboard and test set-up built to prove the concept, measurements and an obtained performance. Both Allan Deviation (AD) and phase difference prove that this concept is highly relevant for Event Horizon Imaging.

II. STATE OF THE ART OSCILLATORS

A quantity of special interest in VLBI is the coherence time [3]. The *approximate* coherence time, Eq. (1) at [3], is that time τ_c for which the rms phase error is 1 radian:

$$2\pi f\ \tau_c\ \sigma_\Sigma(\tau) \approx 1, \qquad (1)$$

where f=557 GHz is the instrument center input frequency, τ is the integration time (in the White Phase Noise region), and $\sigma_\Sigma(\tau)$ is [3]:

$$\sigma_\Sigma(\tau) = \sqrt{\sigma_1^2(\tau) + \sigma_2^2(\tau)} = \sqrt{2}\,\sigma(\tau), \qquad (2)$$

the AD of two independent oscillators embarked on two separate telescope satellites, with $\sigma_1(\tau) = \sigma_2(\tau) = \sigma(\tau)$ being the AD of each oscillator.

The longest integration time is to fall within about 70 s < τ < 450 s, see Eq. (2) at [4]. At the required f=557 GHz, the coherence time (1), (2) provided by two the best H-masers for space, the ACES-ESA active H-maser (AHM), is of only 10 s [Fig. 1]. The coherence time provided by two the iMaser-3000, the best-known ground H-maser, is not much longer, 40 s.

Because the EHI is a future mission concept, the best oscillator (iMaser-3000) performance is referred to compute coherence. Over a short τ, the trend of $\sigma(\tau)$ follows $\tau^{-1/2}$ and

978-1-6654-3935-0/21/$31.00 ©2021 IEEE

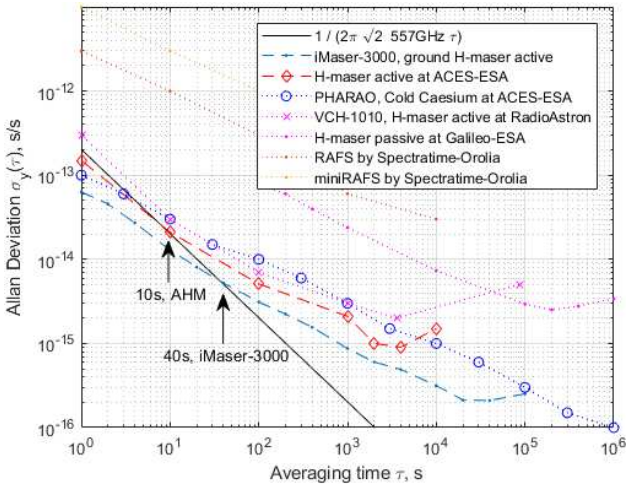

Fig. 1 – Allan Deviation of individual oscillators

the squared product $[\tau\times\sigma_y(\tau)]^2$ is << 1 (see Eq. (18) at [3]) and hence, the coherence efficiency factor β_{WFN} at τ=100 s is

$$\beta_{WFN}(100)=\sqrt{1-\frac{[2\,\pi\,557\,10^9\,100\,\sqrt{2}\,3\,10^{-15}]^2}{6}}=0.78. \quad (3)$$

The interferometer sensitivity budget [1, 4] is not capable to recover this coherence. On the other hand, this budget assumes integration times of up to 450 s, ruling out the use of separate oscillators. Thus, the experimental demonstration of the devised frequency transfer concept is presented in this paper.

III. The Concept Under Test

The concept aims to enable EHI between two (or more) satellites at sub-millimeter wavelength, see Fig. 5 at [2]. Because a phase noise autocorrelation function is free of individual oscillator phases and the argument of this function is self-canceling, the concept under test is phase noise canceling, see Eq. (4) at [5].

The concept block diagram (Fig. 2) is integrated by two twin sets of microwave blocks on board two respective satellites. Oven Controlled Crystal Oscillators (OCXO) are used as master oscillators. The OCXO output tone gets ×M frequency multiplied and sent to the other satellite via a dedicated optical inter-satellite link at point A (B). The tone is received at point A` (B`), slightly offset by a Doppler shift, hence the superscript prime. The concept aims at producing equal sum frequencies at the output of the mixers by adding the frequencies at points A and B` (B and A`); these are A+B`=B+A`. The mixers are configured as up-converters with both IF and LO inputs having about the same frequency and the output having the sum frequency, that is, IF=LO=RF/2. The mixer RF output frequency is then OCXO×M×2. It is further ×N frequency multiplied, providing an *LO frequency output* of OCXO×M×2×N to the interferometer. The difference LO1–LO2 is desired to be null. This would permit EHI satellites to operate with the same Local Oscillator.

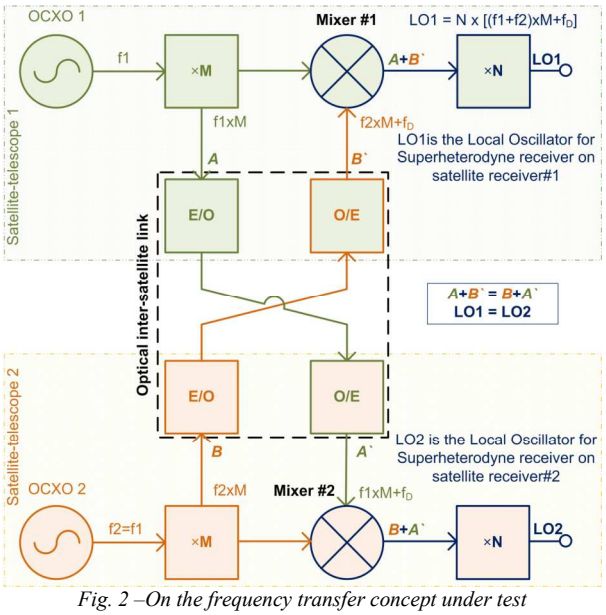

Fig. 2 –On the frequency transfer concept under test

IV. Measurement Set-Up

The measurement setup is integrated by a breadboard under test, performance measurement hardware, and temperature control devices.

A. On Breadboard Development

A large M/N ratio between the frequency multiplication factors (Fig. 2) is desired to mitigate the potential effect of the temperature difference between the EHI satellites. This M/N ratio is constrained by the highest frequency of optoelectronics.

It is also assumed that a PLDRO with the highest-possible output frequency can minimize the number of actual frequency multipliers and amplifiers needed to achieve the ×M factor. Input and output frequencies of PLDRO used for this experiment are 100 MHz and 8.6 GHz, respectively. The PLDRO is based on a Sampling Phase Detector (SPD). This method of phase-locking achieves the lowest phase noise possible besides the theoretical degradation of 20 log N, where N is the multiplication factor. Phase noise degradation is important considering that the aimed instrument frequency is 557 GHz. Additional noise is generated by the driver amplifier, SPD, and loop amplifier. They may all contribute to further degradation in phase noise (typically 3 dB if the OCXO noise floor is -160 dBc/Hz).

It is assumed that a 100 MHz OCXO is preferred over a 10 MHz OCXO followed by a chain of frequency multipliers and power amplifiers.

Optoelectronics employed allows that two LO components are exchanged over a 5 km long fiber (in a spool) using two wavelengths. It has been confirmed that the optoelectronics can operate above the nominal highest frequency of its modulators 18 GHz (iXblue MXER-LN-20), and its performance at 44 GHz is consistent with aimed $\sigma_y(\tau)$ with a margin of about 25 times [5]. A buffer amplifier is needed at the photodetector output to supply enough IF power to the mixer, Fig. 3.

At the output of the mixers, some harmonics are found, like those at a frequency of 2×LO and 2×IF, due to the limited rejection of the mixer, bringing the (unwanted) individual oscillator phase to RF. A double-balanced mixer is adopted as the practical solution to suppress these even harmonics. Marki is the only known supplier of balanced mixers above 50 GHz

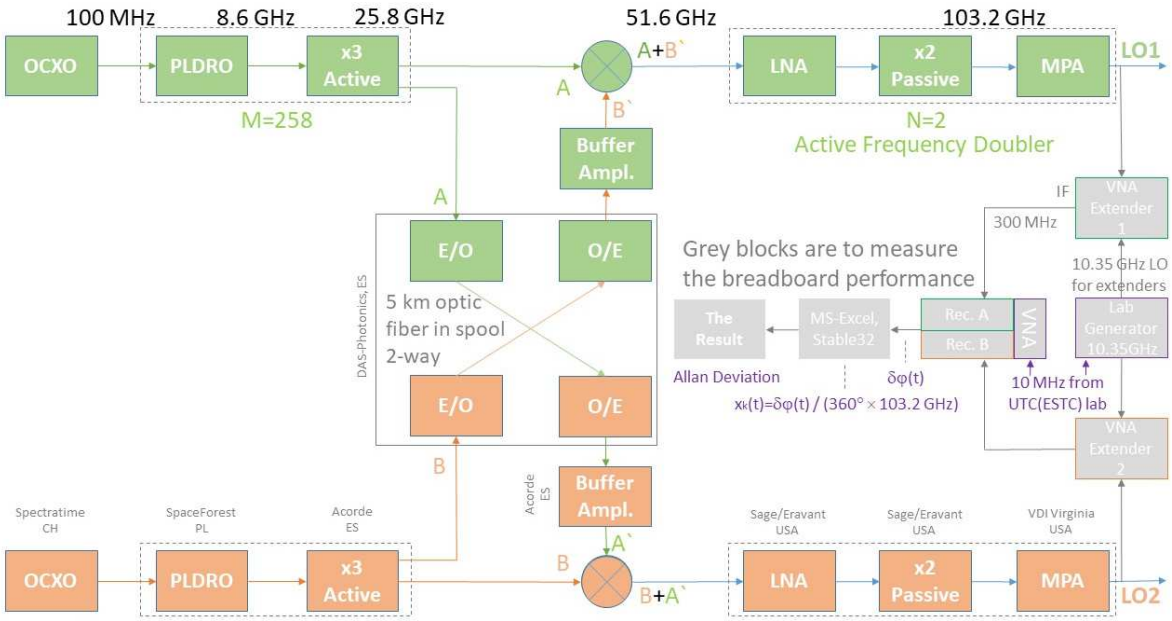

Fig. 3 – The measurement set-up at 103.2 GHz. Branches 1 and 2 are in green and orange, respectively. Grey blocks aren`t part of the breadboard

(the highest RF is 80 GHz) fulfilling the LO=IF=RF/2 condition.

Space heritage on multipliers and amplifiers runs thin above 100 GHz. To make the hardware compatible with a possible follow-on demonstration at a high-frequency radio telescope, the output frequency and power level have to be within 93-121 GHz and 13-18 dBm, respectively [6, 7]. This relaxes the output frequency by a factor of 5 when compared to 557 GHz at the EHI though, medium power amplifiers are still required at 100 GHz outputs (Fig. 3).

The active frequency doubler at the RF output of the mixer has been assembled using COTS amplifiers and a frequency doubler. The list of components is in Table 1.

B. Measurement Approach

The highest frequency of the Miles TimePod 5330, usual hardware to measure the $\sigma(\tau)$, is 30 MHz. Output 103.2 GHz tones are out of band. Another approach is needed to test the concept. A VNA-based measurement approach has been chosen.

The tones under test are input to two (or four) VNA channels. Internally, the VNA receivers down-convert the inputs to an IF band of up to 15 MHz width, sampled at 100 MS/s. The VNA then provides the (unwrapped) phases of incoming signals with respect to the time, at a set-up (nominal) frequency. The measurements were post-processed using Excel and Stable32. Excel is used to calculate both the VNA sampling time and the phase difference. Stable32 has been used to compute the $\sigma(\tau)$. The time error is given by Eq. (6) at [8] as

$$x_k(\tau, t) = \frac{\delta\varphi(\tau,t)}{2\,\pi\, f_0}, \tag{4}$$

where $\delta\varphi(\tau, t)$ is the phase difference between the input tones to the VNA, $\tau = B_{IF}^{-1} = t(i+1) - t(i)$ is the sampling time interval (inverse to the set-up VNA IF bandwidth, as corrected for the VNA digital filter and recording length), and f_0 is the set-up VNA frequency. The measured phase difference is free from the internal phase of either VNA channel (because they are all driven by the same oscillator)

$$\delta\varphi(\tau, t) = \varphi_1(\tau, t) - \varphi_{VNA}(\tau, t) - [\varphi_2(\tau, t) - \varphi_{VNA}(\tau, t)] = \varphi_1(\tau, t) - \varphi_2(\tau, t), \tag{5}$$

where $\varphi_{1.2}(\tau, t)$ are the measured phases in the VNA channels and $\varphi_{VNA}(\tau, t)$ the intrinsic channel phase. The VNA recording is exported to Excel to calculate both the sampling time τ and the time error $x_k(\tau, t)$ in (4). The $x_k(\tau, t)$ has the dimension of time and is a function of time. It can be understood as the phase difference, in time units, between two inputs accumulated over

TABLE I. MICROWAVE ITEMS INTEGRATING THE SET-UP

#	Function	Vendor	Type	Frequency, GHz	pcs
1	Oven Controlled Crystal Oscillator (OCXO)	SpectraTime - Orolia	Low phase noise VHF oscillator	0.1	2
2	Phase-Locked Dielectric Resonator Oscillator (PL DRO)	SpaceForest, PL	PLDRO2	0.1-to-8.6	2
3	Tripler Active with Coupler	Acorde, ES	Triplers X-to-K band (S/N 1,2)	8.6-to-25.8	2
4	Buffer Amplifier	Acorde, ES	Amplifiers K-band (S/N 1,2)	25.8	2
5	Balanced Mixer	Marki, USA	MM1-2567LS	25.8+25.8=51.6	2
6	Low Noise Amplifier	Eravant (SAGE), USA	SBL-4036033080-VFVF-S1	51.6	2
7	Doubler Passive	Eravant (SAGE), USA	SFP-102VF-S2	51.6-to-103.2	2
8	Medium Power Amplifier	VDI, USA	VDI10.0AMP-20-20	103.2	2
9	The set-up includes also Keysight N5227B PNA Microwave Network Analyzer, OML WR-06 extenders driven by Agilent PSG E8267D generator, two spectrum analyzers, and 10 MHz discipline for them. These units are to measure the performance i.e. they are not part of the breadboard.				

a time interval τ. This this $x_k(\tau,t)$ is input to the Stable32 software. The Stable32 computes the $\sigma(\tau)$. The argument of the $\sigma(\tau)$ should not exceed one-tenth of the data set duration as otherwise, the number of $\sigma(\tau)$ which can be computed is too few to provide reliable statistical results, see Eq. (130), (131) at [8]. The measurement approach was validated with Miles TimePod.

C. On a Frequency Offset

The balanced mixers are mixing the local and remote local oscillator signals. The frequency offset

$$\Delta = |IF - LO| \quad (6)$$

between the LO (local LO) and the IF (remote LO) input tones to the mixer establishes the frequency separation between the mixer output signal and unwanted harmonics and hence, the offset Δ affects the $\sigma(\tau)$. At Δ=0, the balanced mixers Marki MM1-2567L offer a 2×LO to RF isolation >30 dB (including the mixer loss). The interferometer maximum frequency can be approximated as (1), (2):

$$f_{max} = \frac{1}{2\pi\,\tau\sqrt{2}\sigma(\tau)}. \quad (7)$$

This Eq. (7) is valid within the trend $\tau\,\sigma(\tau)$=1 (i.e. 1/τ) hence, within the White Phase Noise dominated region of the $\sigma(\tau)$. We have found that an f_{max}=557 GHz is achievable with a frequency offset of Δ=1 kHz with lab generators and up to 1.36 kHz with OCXOs followed by PLDROs. Future optimization of the breadboard may permit to match the 1.1 kHz required to avoid correction for the Doppler residual over the communication link. EHI orbital scenario for water imaging requires 27 Hz instead of 1.1 kHz hence, the need to correct the Doppler residual at this mode. On another hand, the frequency drift of OCXOs due to aging and radiation effects has been accounted for over a mission lifetime of 5 years. The impact of radiation effects is 0.15 Hz, as simulated in SHIELDOSE via SPENVIS, within a worst-case scenario [1]. The expected (maximum overall) frequency drift between the two OCXOs is 280 Hz which translates to *73.2 kHz out of the balanced mixer* due to frequency multiplication from OCXO to the optical ISL. In case a narrower frequency difference is needed, the instant frequency difference can be measured and tuned out by OCXO(s) control voltage. This can be implemented by measuring the "minus" output of the balanced mixer and using this error signal within a feedback loop.

D. The measurement set-up

The standard mixer connection is used to keep the nominal output power. An active frequency doubler (Table 1) is temporarily used without the MPA, at branch#1 (green at Fig. 3).

The 103.2 GHz derived oscillators are beyond a VNA operation frequency band. These oscillators are input to VNA frequency extenders (Table 1). Lab generator drives these extenders at 10.35 GHz. The receiving part of extenders forms 10.35×10=103.5 GHz local oscillators. Extenders are performing frequency down-conversion (103.5-103.2=0.3 GHz). The output from extenders is within the VNA operation frequency band. This permits to use of the selected measurement approach.

Two branches have been installed on contact plates attachable to solid-state thermal controllers. The power consumption is 20 W per branch hence, the dissipated thermal power is below that. The cooling and heating capacities of each thermal controller are 230 W and 420 W, respectively. The test set-up benefits from a ratio(s) between the thermal control capacity and the dissipated thermal power.

V. Measurement Results

A. Phase Difference with respect to the Time

The nominal orbit period is 4.5 hours. Temperature difference within ±3 C represents a relaxed satellite thermal control. We measured that the phase difference between derived 103.2 GHz oscillators follows the set-up temperature difference (Fig. 4). Artifacts at 2.6 and 4.4 hours are generated by operator delays in thermal control.

The phase difference between derived oscillators is the white noise-like function of the time with 1-σ of 0.5° at 103.2 GHz over more than 3 hours, at the same temperature of both branches 22 C (Fig. 5). The phase difference doesn't demonstrate any ramp over hours in the case of normal lab temperature during more than 3 hours (the absent temperature control hence, similar temperatures of branches). The phase difference is also stable in the case of a constant temperature difference of 10 C.

B. Allan Deviation Between 103.2 GHz Oscillators

The $\sigma(\tau)$ measured between two derived 103.2 GHz oscillators during 1.75 hours is $1.1\times10^{-14}/\tau$ over 1,000 s, at Δ=210 kHz (Fig. 6). The $\sigma(\tau)$ degradation towards 1,000 s is an artifact that vanishes in case of a longer measurement time. Moreover, the $\sigma(\tau)$ is the same $1.1\times10^{-14}/\tau$ in all above-mentioned temperature modes of two branches at (a) at a similar temperature, (b) at the same temperature 22°C, (c) at the temperature difference 30–20=10°C constant over measurement time of 2-3 hours, and (d) the temperature difference varying within ±3 C during 4.5 hours.

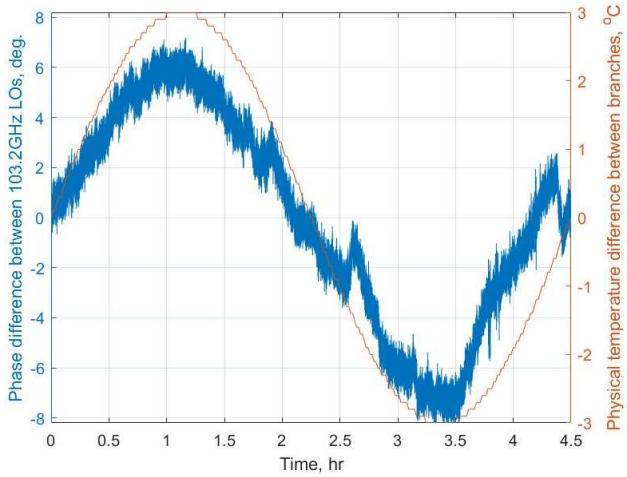

Fig. 4 –Phase difference between two derived 103.2 GHz oscillators with respect to time follows the set-up temperature difference between branches ±3 C during 4.5 hours, being the orbit period

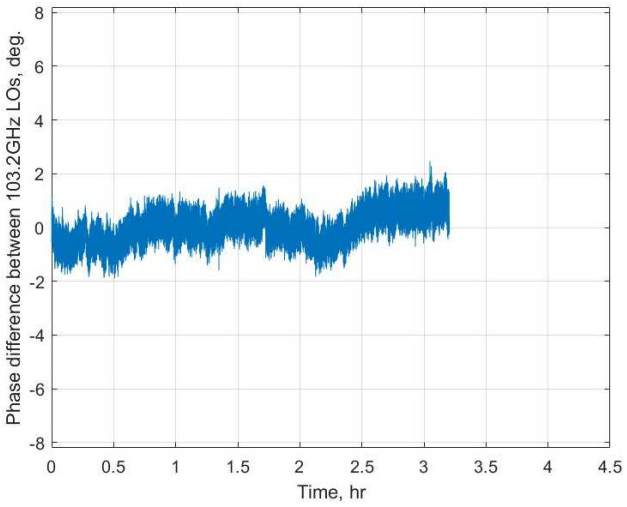

Fig. 5 –Phase difference between two derived 103.2 GHz oscillators with respect to time, at both thermal controllers set to 22 C. Axes are as on Fig. 4 for comparing.

This $\sigma(\tau)$ degrades twice at the maximum EHI system delay (this is the maximum *sum* of communication and geometric delay, see Table 2). The average margin between the degraded performance and the requirement is *11.2 times*. We don't know any other oscillator satisfying this requirement (Fig. 1) and the margin is the advantage. Hence, this is a game-changer for the 3rd generation space Very Long Baseline Interferometry.

As a *verification*, we replaced both OCXO and PLDRO at branch #1 with the lab generator 8.6 GHz (Table 1). The obtained AD $\sigma_\Sigma(\tau)$ at Δ=210 kHz is similar to the previous result $1.1\times10^{-14}/\tau$ and an increase of the Δ to 100 MHz improves the $\sigma_\Sigma(\tau)$ by a factor of 1.22 times which is consistent to increasing of S/N at Fig. 4.

Narrowing the VNA IF bandwidth below 100 Hz improves the $\sigma_\Sigma(\tau)$ by suppressing unwanted interferences hence, indicating that the performance "ceiling" has not been achieved yet. A future improvement, if any, may leverage on analysis of phase noise between these 103.2 GHz oscillators and peaks therein.

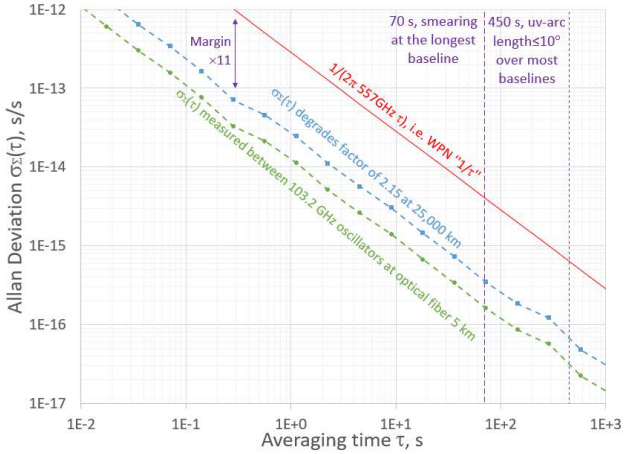

Fig. 6 – The Allan Deviation $\sigma_\Sigma(\tau)$ measured between two derived 103.2 GHz oscillators is $1.1\times10^{-14}/\tau$ over 10 ms<τ<1,000 s

C. The Maximum Frequency

The maximum frequency, $f_{max}(\Delta)$ at Eq. (7), computed from AD $\sigma_\Sigma(\tau)$ measured between derived 103.2 GHz oscillators is on Fig. 7. This function has three characteristic regions namely, the smallest Δ up to 15 kHz featuring many interfering peaks at the worst S/N near 1 kHz, the 15 kHz<Δ<30 kHz featuring a very good performance increase, and the best S/N range Δ>30 kHz. In this set of measurements, we utilized 90 s recordings which constraint the $\sigma_\Sigma(\tau)$ calculated in Stable32 by about 18 s.

D. On Communication Delay

The performance degradation with respect to the inter-satellite link delay has been studied by introducing an artificial delay in post-processing of the VNA recordings.

A four-port VNA has been used to simulate generating of the sum frequency in mixers, which involves two free-running lab generators and the VNA. Different from former cases, the inter-satellite link delays are added *artificially* to the VNA recordings. The longest-possible delays (sum of inter-satellite link delay and science signal geometric delay) are of 0.2 s in EHI and of 16.7 s (5,000,000 km) in ESA's LISA project. Our local oscillator concept has been tested over delays of up to 20 s. It has been observed that the relative phase between the two derived LOs grows linearly with the artificial delay (Fig. 8) at a rate of the order of mHz. There is no frequency discipline between the lab generators used in the experiment. Furthermore, it has been verified that the concept still works well even when there is a large delay asymmetry (between the two directions of the inter-satellite link) of up to 60 m. We didn't test beyond 60 m despite recordings permit doing that.

Using the same technique, the impact of the inter-satellite link delay on the standard deviation σ_ϕ of the phase noise has also been assessed. The lab generators have been disciplined on *two* iMaser-3000 from the ESTEC UTC lab for that. The measurements are given in Table 2. The standard deviation of the phase grew only by a factor 7 over six orders of magnitude increase in the inter-satellite link delay, from 16.7 µs to 16.7 s. This phase change is far smaller than the phase change of each generator.

In the case of the longest baseline of EHI the inter-satellite link delay is of 180 ms and the $\sigma_\Sigma(\tau)$ increases a factor of 2.15 and the phase ramp is smaller than 0.3 mHz.

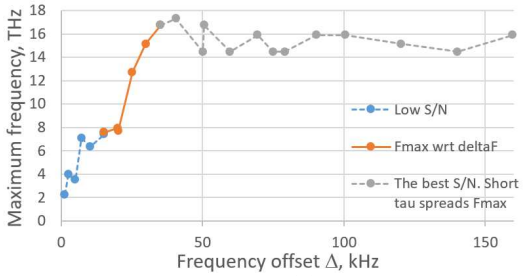

Fig. 7 – The maximum frequency $f_{max}(\Delta)$ for interferometry, computed from Allan Deviation measurements between 103.2 GHz oscillators

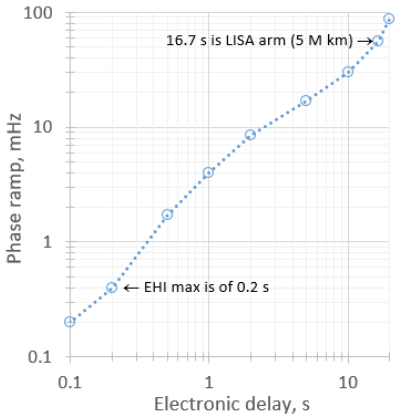

Fig. 8 – The phase ramp between derived LOs at 25.8×2=51.6 GHz

VI. The Attainable Coherence and the Way Forward

The interferometer *coherence* is one of the factors in the sensitivity calculation. The target is to assure the coherence of 0.85 [3], at white phase noise. The achievable coherence varies with respect to the correlator integration time (0.1 s < τ < 450 s) in range of 0.9992–0.9998, at 557 GHz, see Eq.(14), at [3]. Because the $\sigma_Y(\tau)$ degrades twice (Table 2) at the longest baseline 25,000 km, the corresponding coherence degrades to the range of 0.997–0.9992. The ratio of the obtained coherence to a nominal coherence of 0.85 [3] is in the range of 1.17-1.18 that is *useful* for VLBI instrument sensitivity [1, 2, 4].

The concept is proven. Follow-on increase in technology readiness level consists of interferometry utilizing oscillators derived from this concept.

VII. Conclusions

We tested the concept of two-way frequency transfer dedicated to the Event Horizon Imager (EHI) mission concept. We built the breadboard and test set- up, and run tests. A phase difference between derived oscillators is the white noise-like function of the time with 1-σ of 0.5° at 103.2 GHz over more than 3 hours. Varying the temperature difference between branches ±3 C during 4.5 hours, being the orbit period, showed that the phase difference is the function of this temperature difference too. The Allan Deviation measured *between two* derived 103.2 GHz Local Oscillators is 1.1×10^{-14} /τ over 10 ms < τ < 1,000 s; the measurement approach has been verified by Miles TimePod. The EHI coherence requirement for 557 GHz interferometry is satisfied with a margin of 11 times. This factor takes into account the worst performance degradation. Hence, the instrument sensitivity gets useful margin of 17-18%.

TABLE II. *The Phase Noise std σ_ϕ Factor with respect to the Inter-Satellite Link Delay. The Allan Deviation $\sigma(\tau)$ factor is the same to the σ_ϕ factor*

Time delay	std σ_ϕ factor	Note
16.7 us	*1*	*5 km fiber*
89 ms	*1.6*	*EHI ISL Max*
177 ms	*2.15*	*~ EHI Max*
440 ms	*2.9*	*×2 EHI Max*
620 ms	*3.15*	-
796 ms	*3.31*	-
1 s	*3.45*	-
10 s	*6.06*	-
16.7 s	*7.02*	*LISA arm*

The breadboard proves that the concept operates at LISA-ESA scale inter-satellite link delays (up to 20 s) and at a large delay asymmetry of 60 m. The paper provides the current progress on the critical element of the Event Horizon Imager – the local oscillator breadboard.

Acknowledgment

The work was partly supported by the Project NPI-552 *Space-to-space Interferometer System to Image the Event Horizon of the Super Massive Black Hole in the Center of our Galaxy* co-funded by the European Space Agency (ESA) and the Radboud University of Nijmegen (ESA contract 4000122812), by the NWO project PIPP Breakthrough technologies for interferometry in space, and by the microwave lab at the D/TEC of the ESTEC ESA.

Authors are grateful to Microwave Lab at the D/TEC of the ESTEC ESA for hardware and support, to DAS-Photonics (Spain) for optoelectronic hardware, to SpaceForest Ltd. (Poland) for two PLDRO 2 (Phase Locked Dielectric Resonator Oscillators), to AXTAL (Germany) for evaluation boards, to Orolia-SpectraTime (Switzerland), in particular to G. Wagner, for the low noise 100 MHz oscillators and technical support

References

[1] V. Kudriashov et. al., "An Event Horizon Imager (EHI) Mission Concept Utilizing Medium Earth Orbit Sub-mm Interferometry," Chinese Journal of Space Science (CJSS), vol. 41, no. 2, pp. 211 - 233, 2021.

[2] M. Martin-Neira, V. Kudriashov, I. Barat, B. Duesmann, E. Daganzo, "Space-to-space Radio Interferometry System from Medium Earth Orbits," Chinese Journal of Space Science, vol. 39, no. 4, pp. 544 - 562, 2019.

[3] A. E. E. Rogers, J. M. Moran, "Coherence limits for very-long-baseline interferometry," IEEE Transactions on Instrumentation and Measurement, vol. IM-30, no. 4, pp. 283-286, 1981.

[4] F. Roelofs et al., "Simulations of imaging the event horizon of Sagittarius A* from space," Astronomy and Astrophysics, vol. 625, A124, 2019.

[5] V. Kudriashov et. al., "Laboratory demonstration of the local oscillator concept for the Event Horizon Imager," Journal of Astronomical Instrumentation, in press.

[6] F. Mattiocco et al., "Electronically Tuned Local Oscillators for the NOEMA Interferometer," In proc. of: 26th International Symp. on Space Terahertz Technology, P-29, 2015.

[7] V. Kudryashov, "A Bistatic Radiometry System for Object Mapping," Telecommunications and Radio Engineering, vol. 77, iss. 20, pp. 1813 - 1826, 2018.

[8] F. Vernotte, Time and Frequency Metrology, Observatory Theta, Besançon.